RADIATION TRANSPORT BENCHMARKS FOR SIMPLE GEOMETRIES WITH VOID REGIONS USING THE SPHERICAL HARMONICS METHOD

Keisuke Kobayashi*

kobayashi.keisuke@emp.mbox.media.kyoto-u.ac.jp

ABSTRACT

In 2001, an international cooperation on the 3D radiation transport benchmarks for simple geometries with void region was performed under the leadership of E. Sartori of OECD/NEA. There were contributions from eight institutions, where 6 contributions were by the discrete ordinate method and only two were by the spherical harmonics method. The 3D spherical harmonics program FFT3 by the finite Fourier transformation method has been improved for this presentation, and benchmark solutions for the 2D and 3D simple geometries with void region by the FFT2 and FFT3 are given showing fairly good accuracy.

Key Words: Spherical Harmonics Method, 3D Transport Benchmarks, Void Problems, Deterministic Transport Solutions, 3D Multi-Group Transport Equation

1. INTRODUCTION

As the marvelous progress of hardware of computers, the use of the 3-dimensional (3D) radiation transport equations becomes practical problems instead of approximating the system by one or two dimensions. Corresponding to such progress, many 3D transport programs have been developed, and significant efforts for the development of transport calculations were made by OECD/NEA[1, 2].

One of the methods most often used to solve the multi-group transport equation deterministically is the discrete ordinates method[3], which is also called the S_N method. The advantage of this method is that it is easy to make a computer program for arbitrary number of energy groups and S_N orders, since the equation has a simple form. A disadvantage of this method is the phenomenon of the so-called ray effect where the solution shows unphysical oscillations around the true solution for 2D and 3D geometries[4] for systems having large absorption cross section.

On the contrary to the discrete ordinates method, the spherical harmonics method (SHM) has no such difficulty whose lowest approximation is the diffusion equation, since the spherical harmonics function and then the spherical harmonics approximation equations

*Emeritus Professor of Kyoto University Retired from Department of Nuclear Engineering, Kyoto University

Mail Address: 610-1141 Ohe NIshi Shinbayashi Cho 6-7-4, Nishikyoku, Kyoto, Japan

(P_L approximation equations) of the SHM have no specific directions and they are invariant under the rotation of the coordinate system.

It is important for program developers and also for users to know the accuracy of the solution methods and programs, and their applicability for which kind of problems they are preferable, since 3D transport programs are fairly time consuming. For this purpose, many benchmark problems had been proposed, for example by Takeda[5].

As benchmark problems, simple geometries have an advantage that it is easy to obtain exact solution as a reference solution, and further, to improve the accuracy and calculation method than for complicated geometries. Even in the case of simple geometry, it is difficult to obtain good accuracy for the void problems, since there are local high variations of the flux due to the local streaming of radiation.

Ackroyd and Riyait investigated void problems for 2D simple geometries[6]. Extending their problems, 3D radiation transport benchmarks for simple geometry with void region were proposed and promoted by E. Sartori of OECD/NEA[7].

For these benchmarks[8], there were eight contributions, where 6 contributions were by the discrete ordinate method and only two were by the spherical harmonics method of Oliveira et al.[9] and Brown et al.[10]. Many discrete ordinate programs gave very accurate results, since an additional method, a first collision source method was used together with the discrete ordinate method. In the case of pure absorber, this first collision source method gives exact solution.

In the SHM program EVENT by Oliveira et al., the ray tracing method was used in void regions in order to avoid difficulties to use P_L equations in void regions. Therefore, the program EVENT was not a pure SHM program and the equations may not be invariant under the rotation of the coordinates. In the SHM program ARDRA by Brown et al., a fictitious source was added to the true source of the discrete ordinate equations to make them be equivalent to P_L equations, and the resulting discrete ordinate equations were solved like the S_N method.

Although the 3D spherical harmonics program FFT3 based on the finite Fourier transformation method had been developed at that time[11, 12], it was very regrettable that contribution could not be made on account of some program errors in spite of the promotion of Sartori. The FFT3 is improved for the present presentation, and spherical harmonics solutions are given for the 2D void problems given by Ackroyd and Riyait, and for the 3D radiation transport benchmarks for simple geometry with void region.

2. THE SPHERICAL HARMONICS METHOD

The multi-group transport equation to be solved can be written in a form

$$\boldsymbol{\Omega} \cdot \nabla f_g(\boldsymbol{r}, \boldsymbol{\Omega}) + \Sigma_{tg} f_g(\boldsymbol{r}, \boldsymbol{\Omega}) = \int_{4\pi} d\Omega' \Sigma_{sg}(\boldsymbol{\Omega} \leftarrow \boldsymbol{\Omega}') f_g(\boldsymbol{r}, \boldsymbol{\Omega}') + s_g(\boldsymbol{r}, \boldsymbol{\Omega}), \qquad (1)$$

where $f_g(\boldsymbol{r}, \boldsymbol{\Omega})$ is the angular flux of $g-$th group and the direction $\boldsymbol{\Omega}$ at position $\boldsymbol{r}$. Cross sections Σ_{tg} and $\Sigma_{sg}(\boldsymbol{\Omega} \leftarrow \boldsymbol{\Omega}')$ are the total and scattering cross sections from the direction $\boldsymbol{\Omega}'$ to $\boldsymbol{\Omega}$ within the $g-$th group.

The source term $s_g(\boldsymbol{r},\boldsymbol{\Omega})$ includes scattering source from other groups, fission source and external source $s_g^E(\boldsymbol{r},\boldsymbol{\Omega})$;

$$s_g(\boldsymbol{r},\boldsymbol{\Omega}) = \int_{4\pi} d\Omega' \sum_{g'\neq g} \Sigma_s(\boldsymbol{\Omega}, g \leftarrow \boldsymbol{\Omega}', g') f_{g'}(\boldsymbol{r},\boldsymbol{\Omega}') + \frac{\chi_g}{4\pi k} \int_{4\pi} d\Omega' \sum_{g'} \nu\Sigma_{fg'}(\boldsymbol{r}) f_{g'}(\boldsymbol{r},\boldsymbol{\Omega}') + s_g^E(\boldsymbol{r},\boldsymbol{\Omega}). \tag{2}$$

Using the source iteration method, the source term $s_g(\boldsymbol{r},\boldsymbol{\Omega})$ is assumed to be known. For simplicity, the suffix g will be omitted hereafter.

Defining the even and odd parity angular fluxes $f^e(\boldsymbol{r},\boldsymbol{\Omega})$ and $f^d(\boldsymbol{r},\boldsymbol{\Omega})$ by

$$f^e(\boldsymbol{r},\boldsymbol{\Omega}) = \frac{1}{2}\left(f(\boldsymbol{r},\boldsymbol{\Omega}) + f(\boldsymbol{r},-\boldsymbol{\Omega})\right), \quad f^d(\boldsymbol{r},\boldsymbol{\Omega}) = \frac{1}{2}\left(f(\boldsymbol{r},\boldsymbol{\Omega}) - f(\boldsymbol{r},-\boldsymbol{\Omega})\right), \tag{3}$$

Eq.(1) can be rewritten as[13]

$$\boldsymbol{\Omega}\cdot\nabla f^d(\boldsymbol{r},\boldsymbol{\Omega}) + \Sigma_t f^e(\boldsymbol{r},\boldsymbol{\Omega}) = \int_{4\pi} d\Omega' \Sigma_s(\boldsymbol{\Omega}\leftarrow\boldsymbol{\Omega}') f^e(\boldsymbol{r},\boldsymbol{\Omega}') + s^e(\boldsymbol{r},\boldsymbol{\Omega}), \tag{4}$$

$$\boldsymbol{\Omega}\cdot\nabla f^e(\boldsymbol{r},\boldsymbol{\Omega}) + \Sigma_t f^d(\boldsymbol{r},\boldsymbol{\Omega}) = \int_{4\pi} d\Omega' \Sigma_s(\boldsymbol{\Omega}\leftarrow\boldsymbol{\Omega}') f^d(\boldsymbol{r},\boldsymbol{\Omega}') + s^d(\boldsymbol{r},\boldsymbol{\Omega}), \tag{5}$$

where the even and odd parity sources $s^e(\boldsymbol{r},\boldsymbol{\Omega})$ and $s^d(\boldsymbol{r},\boldsymbol{\Omega})$ are defined by the similar equations as Eqs.(3).

We expand the even and odd parity angular fluxes with the spherical harmonics functions $Y_{lm}(\boldsymbol{\Omega})$ as

$$f^e(\boldsymbol{r},\boldsymbol{\Omega}) = \frac{1}{4\pi}\sum_{\substack{l=0\\ \text{even}}}^{L-1}(2l+1)\sum_{m=-l}^{l} f_{lm}(\boldsymbol{r}) Y_{lm}(\boldsymbol{\Omega}), \tag{6}$$

$$f^d(\boldsymbol{r},\boldsymbol{\Omega}) = \frac{1}{4\pi}\sum_{\substack{l=1\\ \text{odd}}}^{L}(2l+1)\sum_{m=-l}^{l} f_{lm}(\boldsymbol{r}) Y_{lm}(\boldsymbol{\Omega}), \tag{7}$$

where the odd order spherical harmonics method, namely odd L is assumed. Assuming that the scattering cross section depends only on $\cos\theta_0 = \boldsymbol{\Omega}\cdot\boldsymbol{\Omega}'$, it can be expressed by the spherical harmonics functions in the form;

$$\Sigma_{sg}(\cos\theta_0) = \frac{1}{4\pi}\sum_{l=0}^{\infty}(2l+1)\Sigma_{slg}\sum_{m=-l}^{l} Y_{lm}(\boldsymbol{\Omega}) Y_{lm}^*(\boldsymbol{\Omega}'). \tag{8}$$

In order to derive the P_L approximation equations concisely, we define a current vector $\boldsymbol{J}(\boldsymbol{r},\boldsymbol{\Omega})$ as

$$\boldsymbol{J}(\boldsymbol{r},\boldsymbol{\Omega}) \equiv \boldsymbol{\Omega} f(\boldsymbol{r},\boldsymbol{\Omega}). \tag{9}$$

We expand this current vector using the spherical harmonics functions as

$$\boldsymbol{J}(\boldsymbol{r},\boldsymbol{\Omega}) \equiv \boldsymbol{\Omega} f(\boldsymbol{r},\boldsymbol{\Omega}) = \frac{1}{4\pi}\sum_{l=0}^{L}(2l+1)\sum_{m=-l}^{l}\boldsymbol{J}_{lm}(\boldsymbol{r})Y_{lm}(\boldsymbol{\Omega}). \tag{10}$$

Expanding the even and odd parity sources $s^e(\boldsymbol{r},\boldsymbol{\Omega})$ and $s^d(\boldsymbol{r},\boldsymbol{\Omega})$ in the same forms as Eqs.(6) and (7) respectively, and substituting these and the scattering cross section of Eq.(8) into Eqs.(4) and (5), we obtain

$$\nabla \boldsymbol{J}^d_{lm}(\boldsymbol{r}) + \Sigma_l f^e_{lm}(\boldsymbol{r}) = s^e_{lm}(\boldsymbol{r}), \tag{11}$$

$$\nabla \boldsymbol{J}^e_{lm}(\boldsymbol{r}) + \Sigma_l f^d_{lm}(\boldsymbol{r}) = s^d_{lm}(\boldsymbol{r}), \tag{12}$$

where $\sum_l = \Sigma_t - \Sigma_{sl}$. The suffixes e and d for f_{lm} and s_{lm} show that l is even and odd, respectively, and for $\boldsymbol{J}_{lm}$, it includes only the moments f^e_{lm} or f^d_{lm}.

Integrating Eqs.(11) and (12) over a small volume around the material interface, we can obtain the boundary condition for the moments at the material interface as

$$\begin{aligned}\boldsymbol{n}\cdot\boldsymbol{J}^d_{lm}(\boldsymbol{r}) \text{ and } \boldsymbol{n}\cdot\boldsymbol{J}^e_{lm}(\boldsymbol{r}) &\text{ are continuous across the material interface}\\ &\text{for even } l \text{ and odd } l, \text{ respectively,}\end{aligned} \tag{13}$$

where $\boldsymbol{n}$ is a unit vector normal to the material interface. The boundary condition of Eq.(13) is reduced in the case of odd order spherical harmonics method to the following condition;

$$\begin{aligned}\boldsymbol{n}\cdot\boldsymbol{J}^d_{lm}(\boldsymbol{r}) \text{ and } f^e_{lm}(\boldsymbol{r}) &\text{ are continuous across the material interface}\\ &\text{for } l = 0, 2, \cdots, L-1, \quad -l \leqq m \leqq l.\end{aligned} \tag{14}$$

This boundary condition of Eq.(14) for the spherical harmonics moments was derived originally by Rumyantsev[14]. In the case of one-dimensional geometry for the $z-$axis direction, for example, the condition of continuity of $\boldsymbol{n}\cdot\boldsymbol{J}^d_{lm}(\boldsymbol{r})$ is reduced to the continuity of the odd order moments $f^d_{lm}(\boldsymbol{r})$. However, in the case of multi-dimensions, the odd order moments $f^d_{lm}(\boldsymbol{r})$ are not continuous across the material interface in general.

Multiplying Eq.(10) by $Y^*_{lm}(\boldsymbol{\Omega})$, integrating it over whole solid angle and using the orthogonality relation, we obtain the moment of the current vector as

$$\begin{aligned}\boldsymbol{J}^e_{lm}(\boldsymbol{r}) &= \int_{4\pi} d\Omega Y^*_{lm}(\boldsymbol{\Omega})\boldsymbol{J}^e(\boldsymbol{r},\boldsymbol{\Omega}) = \int_{4\pi} d\Omega Y^*_{lm}(\boldsymbol{\Omega})\boldsymbol{\Omega} f^e(\boldsymbol{r},\boldsymbol{\Omega})\\ &= \sum_{\substack{l'=0\\ \text{even}}}^{L}\sum_{m'=-l'}^{l'}\boldsymbol{C}^{l'm'}_{lm} f^e_{l'm'}(\boldsymbol{r}),\end{aligned} \tag{15}$$

$$\boldsymbol{J}^d_{lm}(\boldsymbol{r}) = \int_{4\pi} d\Omega Y^*_{lm}(\boldsymbol{\Omega})\boldsymbol{J}^d(\boldsymbol{r},\boldsymbol{\Omega}) = \sum_{\substack{l'=1\\ \text{odd}}}^{L}\sum_{m'=-l'}^{l'}\boldsymbol{C}^{l'm'}_{lm} f^d_{l'm'}(\boldsymbol{r}), \tag{16}$$

where the expansion coefficient $\boldsymbol{C}_{lm}^{l'm'}$ of vector is defined by

$$\boldsymbol{C}_{lm}^{l'm'} = \frac{2l'+1}{4\pi}\int_{4\pi} d\Omega Y_{lm}^*(\boldsymbol{\Omega})\boldsymbol{\Omega}Y_{l'm'}(\boldsymbol{\Omega}). \tag{17}$$

The elements of vector $\boldsymbol{C}_{lm}^{l'm'}$ are given, for example

$$C_{lm1}^{l'm'} = \frac{2l'+1}{4\pi}\int_{4\pi} d\Omega Y_{lm}^*(\boldsymbol{\Omega})\Omega_x Y_{l'm'}(\boldsymbol{\Omega}), \quad C_{lm2}^{l'm'} = \frac{2l'+1}{4\pi}\int_{4\pi} d\Omega Y_{lm}^*(\boldsymbol{\Omega})\Omega_y Y_{l'm'}(\boldsymbol{\Omega}). \tag{18}$$

From Eq.(12), we obtain

$$f_{lm}^d(\boldsymbol{r}) = \frac{1}{\Sigma_l}(-\nabla \boldsymbol{J}_{lm}^e(\boldsymbol{r}) + s_{lm}^d(\boldsymbol{r})). \tag{19}$$

Substituting Eq.(19) into Eq.(16), $\boldsymbol{J}_{lm}^d(\boldsymbol{r})$ is expressed as

$$\boldsymbol{J}_{lm}^d(\boldsymbol{r}) = \sum_{\substack{l'=1\\ \text{odd}}}^{L}\sum_{m'=-l'}^{l'} \boldsymbol{C}_{lm}^{l'm'}\frac{1}{\Sigma_{l'}}(-\nabla \boldsymbol{J}_{l'm'}^e(\boldsymbol{r}) + s_{l'm'}^d(\boldsymbol{r})). \tag{20}$$

Using Eq.(20), Eq.(11) becomes

$$-\nabla\sum_{\substack{l'=1\\ \text{odd}}}^{L}\sum_{m'=-l'}^{l'} \boldsymbol{C}_{lm}^{l'm'}\frac{1}{\Sigma_{l'}}\nabla \boldsymbol{J}_{l'm'}^e(\boldsymbol{r}) + \Sigma_l f_{lm}^e(\boldsymbol{r}) = s_{lm}^e(\boldsymbol{r}) - \sum_{\substack{l'=1\\ \text{odd}}}^{L}\sum_{m'=-l'}^{l'} \boldsymbol{C}_{lm}^{l'm'}\nabla\left(\frac{1}{\Sigma_{l'}}s_{l'm'}^d(\boldsymbol{r})\right), \tag{21}$$

which is written using Eq.(15) as

$$\begin{aligned}-\nabla\sum_{\substack{l'=1\\ \text{odd}}}^{L}\sum_{m'=-l'}^{l'} \boldsymbol{C}_{lm}^{l'm'}\frac{1}{\Sigma_{l'}}\nabla\sum_{\substack{l''=0\\ \text{even}}}^{L}\sum_{m'=-l''}^{l''} \boldsymbol{C}_{l'm'}^{l''m''} f_{l''m''}^e(\boldsymbol{r}) + \Sigma_l f_{lm}^e(\boldsymbol{r})& \\ = s_{lm}^e(\boldsymbol{r}) - \sum_{\substack{l'=1\\ \text{odd}}}^{L}\sum_{m'=-l'}^{l'} \boldsymbol{C}_{lm}^{l'm'}\nabla\left(\frac{1}{\Sigma_{l'}}s_{l'm'}^d(\boldsymbol{r})\right).&\end{aligned} \tag{22}$$

Eq.(22) can be written in the second order differential equations for even order moments $f_{lmg}^e(\boldsymbol{r})$ of a form[15]

$$(-\nabla D_{lm}\nabla + \Sigma_l)f_{lm}^e(\boldsymbol{r}) = \hat{s}_{lm}(\boldsymbol{r}) + \tilde{s}_{lm}(\boldsymbol{r}). \tag{23}$$

Here D_{lm} is a diagonal matrix whose diagonal elements are $D_{lmp}^{l'm'p'}$, $p = p' = 1, 2, 3$, which are defined by

$$D_{lmp}^{l'm'p'} = \sum_{\substack{l''=1\\ \text{odd}}}^{L}\sum_{m''=-l''}^{l''} C_{lmp}^{l''m''}\frac{1}{\Sigma_{l''}}C_{l''m''p'}^{l'm'}, \quad \text{for } p, p' = 1, 2, 3, \tag{24}$$

and

$$\hat{s}_{lm}(\boldsymbol{r}) = s^e_{lm}(\boldsymbol{r}) - \sum_{\substack{l'=1\\ \text{odd}}}^{L} \sum_{m'=-l'}^{l'} \boldsymbol{C}^{l'm'}_{lm} \nabla \left(\frac{1}{\Sigma_{l'}} s^d_{l'm'}(\boldsymbol{r}) \right), \tag{25}$$

$$\tilde{s}_{lm}(\boldsymbol{r}) = \sum_{\substack{l'=0\\ \text{even}}}^{L} \sum_{m'=-l'}^{l'} \sum_{p\neq p'} \sum_{p'\neq p} D^{l'm'p'}_{lmp} \frac{\partial}{\partial x_p} \left(\frac{1}{\Sigma_{l'}} \frac{\partial}{\partial x_{p'}} f^e_{l'm'}(\boldsymbol{r}) \right), \tag{26}$$

where $x_1 = x, x_2 = y$ etc.

Eqs.(23) have the same form as the diffusion equation, and they can be solved by approximating them in the discrete form for the space variables using the box integration method. They were solved from the lower order to higher moments, namely from $(l, m) = (0, 0)$ to $(l, m) = (2, 0)$, $(l, m) = (2, 1)$ etc., and higher moments thus obtained were substituted successively to the right side of the equations, which can be called as the middle iteration, since this iteration was done between the inner and the source iterations.

The $(l, m) = (0, 0)-$th equation of the left side of Eq.(23) is just the same as the usual diffusion equation, and the additional terms of the right side to the source terms are contribution from the higher moments which correct the total flux becomes exact. These additional terms from the higher moments become larger as the deviation of the diffusion equation from exact value are larger. Applying the box integration method to Eq.(23), PLXY[15] and PLXYZ programs[16, 17] were developed for x-y and x-y-z geometries, respectively.

3. FINITE FOURIER TRANSFORMATION

We assume that cross sections are piecewise constant in space. Multiplying Eq.(11) by $e^{-i\boldsymbol{kr}}$ and integrating it over a finite region V in which cross sections are constant, we obtain

$$i\boldsymbol{k}\boldsymbol{J}^d_{lm}(\boldsymbol{k}) + \int_S dS e^{-i\boldsymbol{kr}} \boldsymbol{n} \cdot \boldsymbol{J}^d_{lm}(\boldsymbol{r}) + \Sigma_l F^e_{lm}(\boldsymbol{k}) = S^e_{lm}(\boldsymbol{k}), \tag{27}$$

where S is a surface of the region V and $\boldsymbol{n}$ is a unit vector normal to the surface S, and the finite Fourier transform in a finite region V using a transformation parameter $\boldsymbol{k}$ are defined by

$$\mathcal{F}(f_{lm}(\boldsymbol{r})) \equiv F_{lm}(\boldsymbol{k}) = \int_V d\boldsymbol{r} e^{-i\boldsymbol{kr}} f_{lm}(\boldsymbol{r}), \tag{28}$$

$$\mathcal{F}(s_{lm}(\boldsymbol{r})) \equiv S_{lm}(\boldsymbol{k}) = \int_V d\boldsymbol{r} e^{-i\boldsymbol{kr}} s_{lm}(\boldsymbol{r}), \tag{29}$$

$$\mathcal{F}(\boldsymbol{J}_{lm}(\boldsymbol{r})) \equiv \boldsymbol{J}(\boldsymbol{k}) = \int_V d\boldsymbol{r} e^{-i\boldsymbol{kr}} \boldsymbol{J}_{lm}(\boldsymbol{r}). \tag{30}$$

Similarly from Eqs.(12), (15) and (16), we obtain

$$i\boldsymbol{k}\boldsymbol{J}^e_{lm}(\boldsymbol{k}) + \int_S dS e^{-i\boldsymbol{kr}} \boldsymbol{n} \cdot \boldsymbol{J}^e_{lm}(\boldsymbol{r}) + \Sigma_l F^d_{lm}(\boldsymbol{k}) = S^d_{lm}(\boldsymbol{k}), \tag{31}$$

$$\boldsymbol{J}^e_{lm}(\boldsymbol{k}) = \sum_{\substack{l'=0\\ \text{even}}}^{L} \sum_{m'=-l'}^{l'} \boldsymbol{C}^{l'm'}_{lm} F^e_{l'm'}(\boldsymbol{k}), \qquad \boldsymbol{J}^d_{lm}(\boldsymbol{k}) = \sum_{\substack{l'=1\\ \text{odd}}}^{L} \sum_{m'=-l'}^{l'} \boldsymbol{C}^{l'm'}_{lm} F^d_{l'm'}(\boldsymbol{k}). \tag{32}$$

From Eq.(31), we obtain

$$F^d_{lm}(\boldsymbol{k}) = \frac{1}{\Sigma_l}\left(-i\boldsymbol{k}\boldsymbol{J}^e_{lm}(\boldsymbol{k}) - \int_S dS e^{-i\boldsymbol{k}\boldsymbol{r}}\boldsymbol{n}\cdot\boldsymbol{J}^e_{lm}(\boldsymbol{r}) + S^d_{lm}(\boldsymbol{k})\right). \tag{33}$$

Substituting Eq.(33) into Eq.(32), $\boldsymbol{J}^d_{lm}(\boldsymbol{r})$ is expressed as

$$\boldsymbol{J}^d_{lm}(\boldsymbol{k}) = \sum_{\substack{l'=1\\ \text{odd}}}^{L} \sum_{m'=-l'}^{l'} \boldsymbol{C}^{l'm'}_{lm} \frac{1}{\Sigma_{l'}}\left(-i\boldsymbol{k}\boldsymbol{J}^e_{l'm'}(\boldsymbol{k}) - \int_S dS e^{-i\boldsymbol{k}\boldsymbol{r}}\boldsymbol{n}\cdot\boldsymbol{J}^e_{l'm'}(\boldsymbol{r}) + S^d_{l'm'}(\boldsymbol{k})\right). \tag{34}$$

Using Eq.(34), Eq.(27) becomes

$$-i\boldsymbol{k}\sum_{\substack{l'=1\\ \text{odd}}}^{L} \sum_{m'=-l'}^{l'} \boldsymbol{C}^{l'm'}_{lm} \frac{1}{\Sigma_{l'}}\left(i\boldsymbol{k}\boldsymbol{J}^e_{l'm'}(\boldsymbol{k}) + \int_S dS e^{-i\boldsymbol{k}\boldsymbol{r}}\boldsymbol{n}\cdot\boldsymbol{J}^e_{l'm'}(\boldsymbol{r})\right) + \int_S dS e^{-i\boldsymbol{k}\boldsymbol{r}}\boldsymbol{n}\cdot\boldsymbol{J}^d_{lm}(\boldsymbol{r})$$

$$+\Sigma_l F^e_{lm}(\boldsymbol{k}) = S^e_{lm}(\boldsymbol{k}) - \sum_{\substack{l'=1\\ \text{odd}}}^{L} \sum_{m'=-l'}^{l'} \boldsymbol{C}^{l'm'}_{lm} i\boldsymbol{k}\frac{1}{\Sigma_{l'}} S^d_{l'm'}(\boldsymbol{k}), \tag{35}$$

which can be written using Eqs.(15) and the first equation of (32),

$$-i\boldsymbol{k}\sum_{\substack{l'=1\\ \text{odd}}}^{L} \sum_{m'=-l'}^{l'} \boldsymbol{C}^{l'm'}_{lm} \frac{1}{\Sigma_{l'}} i\boldsymbol{k}\sum_{\substack{l''=0\\ \text{even}}}^{L} \sum_{m''=-l''}^{l''} \boldsymbol{C}^{l''m''}_{l'm'} F^e_{l''m''}(\boldsymbol{k})$$

$$-i\boldsymbol{k}\sum_{\substack{l'=1\\ \text{odd}}}^{L} \sum_{m'=-l'}^{l'} \boldsymbol{C}^{l'm'}_{lm} \frac{1}{\Sigma_{l'}} \sum_{\substack{l''=0\\ \text{even}}}^{L} \sum_{m''=-l''}^{l''} \int_S dS e^{-i\boldsymbol{k}\boldsymbol{r}}\boldsymbol{n}\boldsymbol{C}^{l''m''}_{l'm'} f^e_{l'm'}(\boldsymbol{r})$$

$$+\int_S dS e^{-i\boldsymbol{k}\boldsymbol{r}}\boldsymbol{n}\cdot\boldsymbol{J}^d_{lm}(\boldsymbol{r}) + \Sigma_l F^e_{lm}(\boldsymbol{k}) = S^e_{lm}(\boldsymbol{k}) - \sum_{\substack{l'=1\\ \text{odd}}}^{L} \sum_{m'=-l'}^{l'} \boldsymbol{C}^{l'm'}_{l''m} i\boldsymbol{k}\frac{1}{\Sigma_{l'}} S^d_{l'm'}(\boldsymbol{k}). \tag{36}$$

Eq.(36) can be rewritten

$$\left(\sum_{p=1}^{3} D^{lmp}_{lmp} k_p^2 + \Sigma_l\right) F^e_{lm}(\boldsymbol{k}) - \sum_{p=1}^{3} D^{lmp}_{lmp} i k_p \int_S dS n_p e^{-i\boldsymbol{k}\boldsymbol{r}} f^e_{lm}(\boldsymbol{r})$$

$$+\int_S dS e^{-i\boldsymbol{k}\boldsymbol{r}}\boldsymbol{n}\cdot\boldsymbol{J}^d_{lm}(\boldsymbol{r}) = \hat{S}_{lm}(\boldsymbol{k}) + \tilde{S}_{lm}(\boldsymbol{k}), \tag{37}$$

which corresponds with Eq.(23), where

$$\hat{S}_{lm}(\boldsymbol{k}) = S^e_{lm}(\boldsymbol{k}) - \sum_{\substack{l'=1\\ \text{odd}}}^{L} \sum_{m'=-l'}^{l'} \boldsymbol{C}^{l'm'}_{lm} i\boldsymbol{k}\frac{1}{\Sigma_{l'}} S^d_{l'm'}(\boldsymbol{k}). \tag{38}$$

$$\tilde{S}_{lm}(\boldsymbol{k}) = -\sum_{\substack{l'=0\\ \text{even}}}^{L} \sum_{m'=-l'}^{l'} \sum_{p\neq p'} \sum_{p'\neq p} D^{l'm'p'}_{lmp} k_p \frac{1}{\Sigma_{l'}} k_{p'} F^e_{l'm'}(\boldsymbol{k}), \tag{39}$$

where $k_1 = k_x, k_2 = k_y$ etc.

We apply the condition for the transformation constant $\boldsymbol{k}$ such that the following condition holds:

$$\sum_{p=1}^{3} D_{lmp}^{lmp} k_p^2 + \Sigma_l = 0. \tag{40}$$

Using Eq.(40), we obtain an integral equation for the flux and current at the material interface from Eq.(37),

$$-\sum_{p=1}^{3} D_{lmp}^{lmp} i k_p \int_S dS n_p e^{-i\boldsymbol{kr}} f_{lm}^e(\boldsymbol{r}) + \int dS e^{-i\boldsymbol{kr}} \boldsymbol{n} \cdot \boldsymbol{J}_{lm}^d(\boldsymbol{r}) = \hat{S}_{lm}(\boldsymbol{k}) + \tilde{S}_{lm}(\boldsymbol{k}). \tag{41}$$

The left side of Eq.(41) contains only the boundary values of the flux and current, and they are just the values which should be continuous across the boundary in the spherical harmonics method as shown in Eq.(14). Then 2D and 3D problems can be solved as 1D and 2D problems respectively, since boundaries of 2D and 3D are 1D and 2D respectively.

Expanding SH moments $f_{lmg}^e(\boldsymbol{r})$ at the region boundary in Fourier series of space variables and retaining only the first term, we can obtain 3-points finite difference like equations for $x-$, $y-$ and $z-$ axis directions, which can be solved using the alternating direction inner iteration. FFT2[18] and FFT3 programs[11, 12] were developed for 2D $x-y$ and 3D $x-y-z$ geometries.

4. NUMERICAL RESULTS

4.1. 2D Void Problem

Ackroyd and Riyait[6] investigated flux distributions for 2D void problems of three simple geometries extensively. In Fig.1 is shown the geometry for the dog-leg duct one group source problem given by Ackroyd and Riyait, where the dog-leg duct region is void. Cross sections $\Sigma_t = \Sigma_a = 0.5\text{cm}^{-1}$ and $\Sigma_t = \Sigma_a = 0.005\text{cm}^{-1}$ are used for shield and void regions, respectively.

Since only the reflective or zero flux boundary conditions at the outer most boundary in the SHM programs PLXY and FFT2 can be used, pure absorber of the thickness of 5cm having the same absorption cross section as the shield is added beyond the vacuum boundary and zero flux condition is used.

In Figs.(2) and (3) are shown the total flux on the $x-$axis OX at $y = 0$ of Fig.(1) by the PLXY and FFT2 programs from P_3 to P_9 approximations respectively, and in Fig.(4) are given the total fluxes by P_9 approximation by PLXY[19] and FFT2. The dot points are given by Ackroyd et al. as RANKERN and can be regarded as exact.

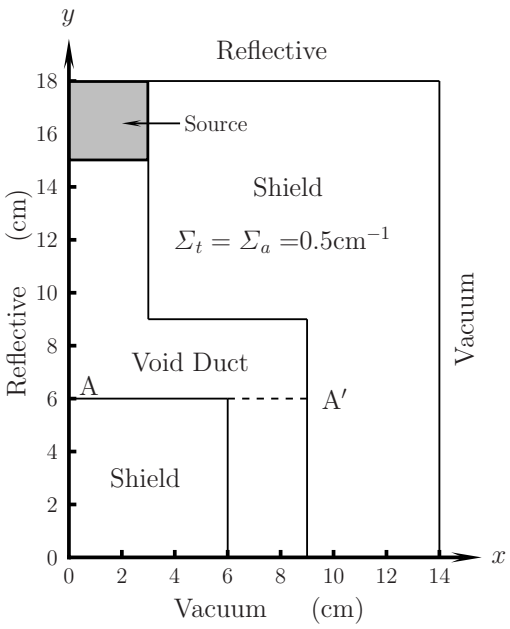

Fig.1 Problem 3: Geometry for the dog-leg duct source problem

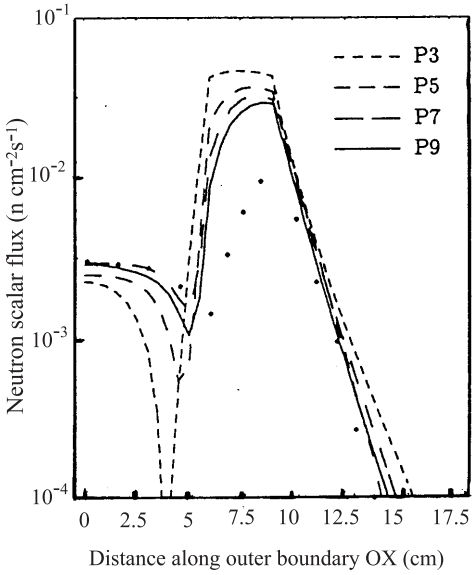

Fig.2 Total flux by RANKERN · given by Ackroyd et al. and the PLXY along outer boundary OX

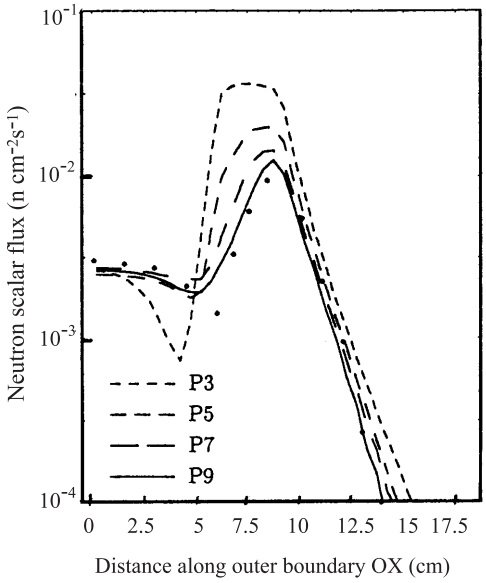

Fig.3 Total flux by RANKERN · and the FFT2 along outer boundary OX

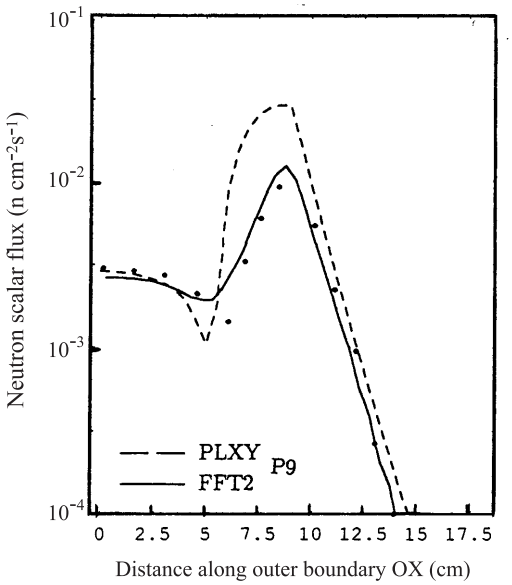

Fig.4 Total flux by RANKERN ·, the PLXY and FFT2 with P_9 along outer boundary OX

It is seen clearly that the flux distributions by the PLXY do no approach to the exact values of RANKERN, whereas those by the FFT2 converge to the values of RANKERN as the order of P_L approximation increases. These improvements of accuracy of the flux distributions by FFT2 may be due to the fact that the rigorous boundary conditions of Eq.(14) at the material interface are satisfied. This means that it is important to obtain good accuracy for the boundary condition of Eq.(14) to be satisfied in void problems, although both programs give the same accuracy for homogeneous or nearly homogeneous problems.

4.2. 3D Radiation Transport Benchmark Problems for Simple Geometries with Void Region

The geometry of the dog leg void duct problem of the 3D benchmarks for simple geometries with void regions[7] is shown in Figs.5 and 6. For this problem, the vacuum boundary condition was simulated by adding pure absorber of thickness of 50cm having the same absorption cross section as in Region 3 to the outer most boundary and using zero flux condition as done in the FFT2. In Fig.7 are shown the total fluxes at $y = 95$cm, and $z = 25$cm on the points shown in Fig.5 in $x-$axis direction by the P_7 using the mesh width of 10/7cm=1.43cm by FFT3[†], and in Fig.8, the relative values to the exact flux.

The accuracy of FFT3 by the P_7 seems better than the EVENT P_9 by Oliveira et al. and nearly the same as ARDRA by Brown et al., where P_{21} approximations was used. The reason to use such high order may be due to the boundary condition used by ARDRA at the material interface. In the S_N method, the continuity condition of the angular flux is used, although in the SHM, the boundary condition of Eq.(14) should be used. Namely, the use of the continuity condition of the angular flux is not equivalent to the boundary condition of Eq.(14).

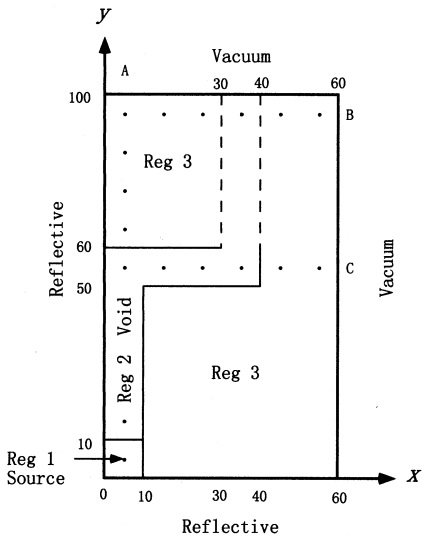

Fig.5 $x-y$ plane of Problem 3, Shield with dog leg void duct

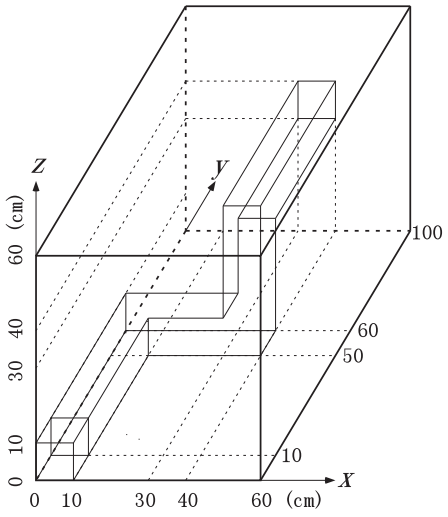

Fig.6 Sketch of Problem 3, Shield with dog leg void duct

[†]Computations were done using Windows Xp PC

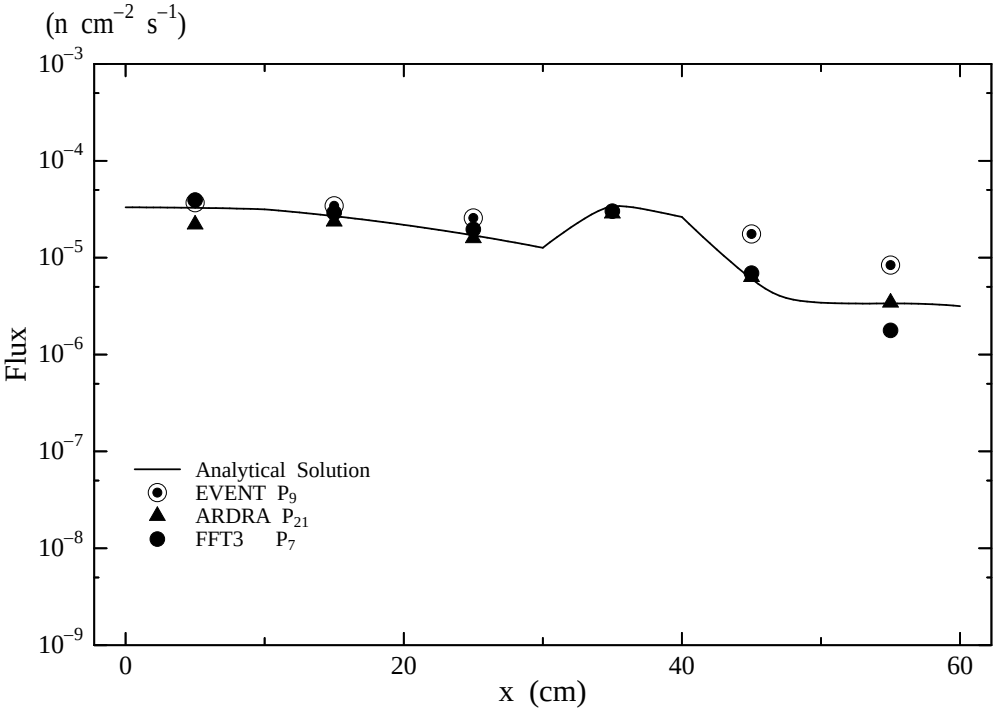

Fig.7 Total flux at $y = 95$cm, and $z = 25$cm on the points shown in Fig.5 in $x-$axis direction

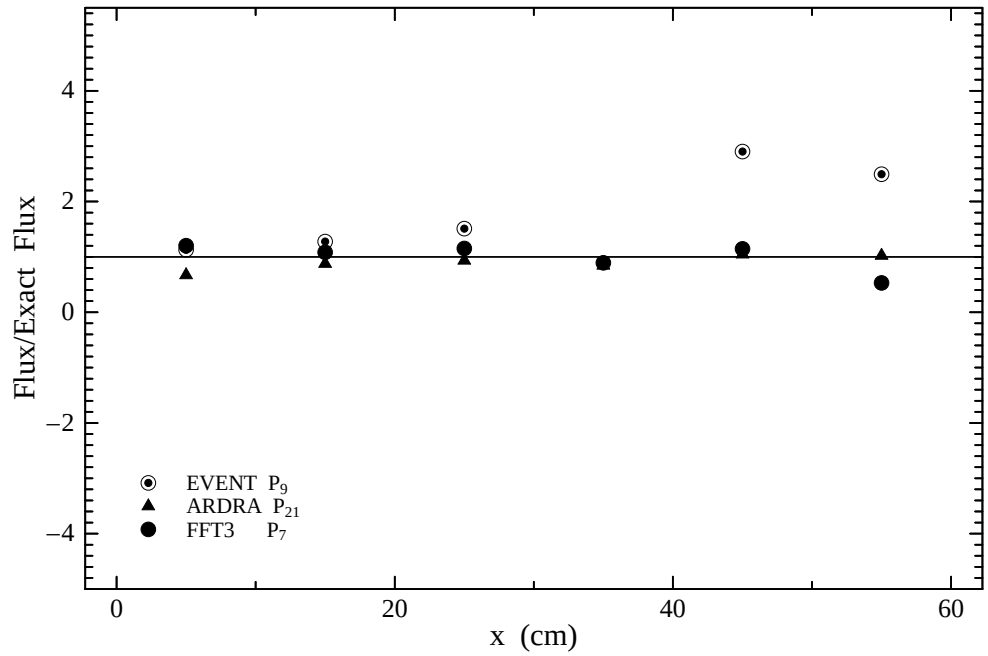

Fig.8 C/E for the total flux of Fig.7

In the present one group problem, there are two iterations, the inner and middle iterations. There is a difficulty of the slow convergence of the middle iteration for FFT3, although there is no such difficulty for FFT2. If the error criterion of the inner iteration is not sufficiently small, there is even a possibility of the divergence of the middle iteration. For the practical use of the FFT3, further work for improvement of the iteration method is necessary.

5. CONCLUSION

Numerical calculations show that the solution of the finite difference equations by PLXY for the 2nd order differential equations of the P_L equations does not converge to the exact solution as the order of L increases, whereas solutions of the P_L equations of FFT2 and FFT3 derived using the finite Fourier transformation method converge to the exact solution.

The difference between programs PLXY, PLXYZ and FFT2, FFT3 is in that the rigorous material boundary conditions for the SHM are used explicitly in the FFT2 and FFT3, however, they are not used explicitly in PLXY and PLXYZ. Namely, the FFT method has an advantage that the boundary conditions for SHM can be used explicitly and gives higher accuracy. However, it is desirable further work for the development of the acceleration method of the iteration calculations.

ACKNOWLEDGEMENTS

The author wishes to express his sincere thanks to E. Sartori for his leadership for the development of 3D Transport programs and 3D Benchmark projects. He thanks also the participants for their international cooperation with the Radiation Transport Benchmarks for Simple Geometries with Void Regions.

REFERNCES

1. E. Sartori et al., "3-D Deterministic Radiation Transport Computer Programs. Features, Applications and Perspectives", OECD Proceedings, Nuclear Energy Agency (1997).
2. B.D.Ganapol, "Analytical Benchmarks for Nuclear Engineering Applications Case Studies in Neutron Transport Theory", Nuclear Energy Agency, OECD, 2008. NEA/DB(2008)1, NEA No: 6292.
3. Edited by H. Greenspan, C.N. Kelber, and D. Okrent, Computing Methods in Reactor Physics, Chap.3 Transport Theory, The Method of Discrete Ordinates, by B.G. Carlson and K.D. Lathrop, Gordon and Breach Science Publishers (1968).
4. K.D. Lathrop, "Ray Effects in Discrete Ordinates Equations", Nucl. Sci. Eng., **32**, pp.357-369 (1968).
5. T. Takeda, and H. Ikeda, "*3-D Neutron Transport Benchmarks*", NEACRP-L-330 (1991).
6. R.T. Ackroyd and N.S. Riyait, "Iteration and Extrapolation Method for the Approximate Solution of the Even-Parity Transport Equation for Systems with Voids", Ann. nucl. Energy, **16**, pp.1-32 (1989).

7. K. Kobayashi, "A Proposal for 3D Radiation Transport Benchmarks for Simple Geometries with Void Region, " 3-D Deterministic Radiation Transport Computer Programs, OECD Proceedings, pp.403-410 (1996).
8. E. Sartori and K.Kobayashi, Guest Editors, " 3-D Radiation Transport Benchmark Problems for Simple Geometries with Void Region", Progress in Nucl. Energy, **39**, pp.119-284 (2001).
9. C.R.E. Oliveira, M.D. Eaton and A.P. Umpleby, et al. "Finite Element-Spherical Harmonics Solutions of the 3D Kobayashi Benchmarks with Ray-Tracing Void Treatment", Progress in Nucl. Energy, ibid. pp.243-261 (2001).
10. P.N. Brown, B. Chang and U.R. Hanebutte, "Spherical Harmonic Solutions of the Boltzmann Transport Equation via Discrete Ordinates", Progress in Nucl. Energy, ibid. pp.263-284 (2001).
11. K. Kobayashi, H. Kikuchi and K. Tsutuguchi, "Solution of Multigroup Transport Equation in $x-y-z$ Geometry by the Spherical Harmonics Method using Finite Fourier Transformation", J. Nucl. Sci. Technol. **30**, pp.31-47 (1993).
12. K. Kobayashi, "On the Advantage of the Finite Fourier Transformation Method for the Solution of a Multigroup Transport Equation by the Spherical Harmonics Method", Transp. Theory Statis. Phys. **24**, pp.113-132 (1995).
13. K. Kobayashi "3D Spherical Harmonics Code FFT3 by the Finite Fourier Transformation Method", pp.141-154, 3-D Deterministic Radiation Transport Computer Programs, OECD Proceedings, OECD/NEA (1997).
14. G. Ya. Rumyantsev, "Boundary conditions in the spherical harmonic method", J. Nucl. Energy, Parts A/B, **16**, pp.111-118 (1962).
15. K. Kobayashi, H. Ohigawa and H. Yamagata, "The Spherical Harmonics Method for the Multi-Group Transport Equation in $x-y$ Geometry", Ann. nucl. Energy, **13**, pp.663-678 (1986).
16. S. Fujiwara, "P_L Solutions of Three-Dimensional Multi-Group Transport Equation", Diploma Thesis, Department of Nuclear Engineering, Kyoto University (1988).
17. H. Makigami, "Solution of Three-Dimensional Multi-Group Transport Equation", Diploma Thesis, Department of Nuclear Engineering, Kyoto University (1988).
18. K. Kobayashi and N. Hiyama, "Finite Fourier Transformation and its Application to the Solution of Multigroup Transport Equation in $x-y$ Geometry by the Spherical Harmonics Method", Proc. Int. Conf. on Physics of Reactors, XII-29, Marseille, France, Apr. 23 (1990).
19. H. Sakaguchi, "Approximate Solution of transport equation for void system", Master thesis, Department of Nuclear Engineering, Kyoto University (1996).